International Journal of GEOMATE
(Geotechnique, Construction Materials and Environment)
ISSN: 2186-2982 (P), 2186-2990 (O), Japan
Vol. 31, Issue 145, September 2026, pp.57-65; DOI: 10.21660/2026.145.5624

GEOTECHNICAL PARAMETER ANALYSIS OF LANDSLIDE-PRONE AREAS USING MASW AND SEISMIC REFRACTION

*Muhammad Syukri[1,2], Zul Fadhli[2], Purwandy Hasibuan[3], Nordiana Binti Mohd Muztaza[4] and Haris Saputra[5]

[1]Department of Physics, Faculty of Mathematics and Natural Sciences, Universitas Syiah Kuala, Indonesia
[2]Department of Geophysics Engineering, Faculty of Engineering, Universitas Syiah Kuala, Indonesia
[3]Department of Civil Engineering, Faculty of Engineering, Universitas Syiah Kuala, Indonesia
[4]Geophysics Program, School of Physics, Universiti Sains Malaysia, Pulau Pinang, Malaysia
[5]Department of Civil Engineering, Faculty of Engineering, Universitas Muhammadiyah Aceh, Indonesia

*Corresponding Author, Received: 24 April 2026, Revised: 21 May 2026, Accepted: 26 May 2026

ABSTRACT: National transportation routes in the Seulawah region frequently experience damage due to external factors, particularly intense rainfall and seismic activity associated with the Seulimum fault. These impacts often trigger geohazards such as landslides, subsidence, and road deformation, which are strongly related to weak subsurface geotechnical conditions. This study aims to characterize the geotechnical properties of subsurface materials along the Seulawah route by integrating seismic refraction and Multichannel Analysis of Surface Waves (MASW) methods. Data acquisition was conducted using PASI 16S24-N instruments at two survey locations, with two seismic refraction lines and two MASW lines at each site, and a geophone spacing of 2 meters. Data processing was performed using Seisimager and PlotRefa software to generate compressional wave velocity (Vp) and shear wave velocity (Vs) models. The results indicate that the upper layer, at a depth of approximately 8–11 m, is characterized by low Vp (295–1000 m/s) and Vs (112–350 m/s) values, low density (1.73–1.86 g/cm³), and low bearing capacity (1.94–4.87), suggesting soft and unstable materials. In contrast, the second layer exhibits significantly higher geomechanical properties, with Vp reaching 2411 m/s, Vs up to 897 m/s, density ranging from 2.14 to 2.92 g/cm³, and bearing capacity of 26.23, indicating dense volcanic materials such as tuff or breccia. These findings demonstrate a clear transition from weak surface layers to more competent subsurface formations and confirm that the integration of seismic refraction and MASW methods provides an effective approach for detailed geotechnical characterization in landslide-prone areas.

Keywords: Landslide Hazard, Geotechnical Characterization, MASW, Seismic Refraction, Subsurface Investigation.

1. INTRODUCTION

Landslides are a recurring natural hazard along the Seulawah highway in Aceh, causing significant infrastructure damage and economic disruption. This road serves as a primary transportation corridor connecting the capital of Aceh Province with surrounding regions. The Seulawah area is characterized by steep mountainous terrain composed predominantly of volcanic tuff deposits [1]. These materials play a critical role in slope instability due to their high porosity, which promotes water absorption and saturation, thereby increasing unit weight and driving forces [2]. In addition, tuff is highly susceptible to weathering and alteration into kaolinite clay, which exhibits swelling–shrinkage behavior that further reduces slope stability [3, 4].

Geologically, the Seulawah Hills are influenced by the subduction of the Indo-Australian plate beneath the Eurasian plate, with a convergence rate of 5–7 cm/year [5]. This tectonic interaction forms the Sumatra fault system, a major NW–SE trending dextral strike-slip fault extending approximately 1,900 km [6]. One of its active segments, the Seulimum segment, accommodates lateral deformation and contributes to regional uplift, producing steep slopes and rugged topography [7, 8]. Seismic activity associated with this fault system further exacerbates slope instability, particularly in areas dominated by weathered Quaternary deposits [9]. Consequently, morphotectonic processes in the region significantly increase geological vulnerability.

Variations in lithology, fragmentation, and deformation result in heterogeneous subsurface conditions with contrasting physical and mechanical properties [10]. These contrasts strongly influence slope stability and can be effectively investigated using integrated geotechnical and geophysical approaches. Near-surface geophysical methods, such as electrical resistivity, seismic wave velocity, and density-based analysis, have been widely applied to characterize subsurface conditions in landslide-prone areas [11, 12, 13]. Previous studies have demonstrated the application of resistivity and seismic methods to identify weak zones, slip surfaces, and subsurface structures associated with landslides [14 - 18].

Among these methods, the Multichannel Analysis of Surface Waves (MASW) is widely recognized as an effective non-destructive technique for characterizing near-surface shear-wave velocity (Vs) structures [19]. MASW has been successfully applied to identify subsurface layering and potential slip planes [20, 21]. However, previous studies generally focused on limited geotechnical parameters, such as density or bearing capacity, or on subsurface imaging alone, leaving the integrated estimation of multiple engineering and geotechnical parameters insufficiently explored [22 - 25].

Therefore, this study aims to provide a more comprehensive geotechnical characterization by integrating MASW and seismic refraction methods. The combined Vp and Vs data are utilized to derive key engineering parameters, including Young's modulus, bulk modulus, shear modulus, and Poisson's ratio [26–29], as well as geotechnical parameters such as stress ratio, density, and bearing capacity [24, 30, 31]. Unlike previous studies, this integrated approach simultaneously estimates multiple engineering and geotechnical parameters to improve subsurface characterization and provide a more reliable basis for landslide hazard assessment and mitigation in the Seulawah area.

2. RESEARCH SIGNIFICANCE

This study introduces an integrated geophysical–geotechnical framework that simultaneously utilizes MASW- and seismic refraction-derived Vs and Vp data to quantify a comprehensive set of engineering and geotechnical parameters. By integrating both seismic methods rather than evaluating individual parameters separately, the proposed framework enables more reliable identification of weak zones and subsurface mechanical contrasts in volcanic terrains. The proposed approach improves the resolution of weak zone detection and subsurface layering. It provides a transferable and cost-effective strategy for enhancing landslide hazard assessment and supports more reliable infrastructure design in tectonically active regions.

3. DATA AND METHOD

3.1 Geological Setting

The study area is located in a mountainous region with steep slopes and high landslide susceptibility along the Seulawah highway. Landslides frequently occur during the rainy season due to the combined influence of rainfall, geological structures, and human activities. The regional geological map (Fig. 1) shows that the site is part of the Lam Teuba Formation (QTvt), dominated by volcanic materials such as andesite, dacite, tuff,

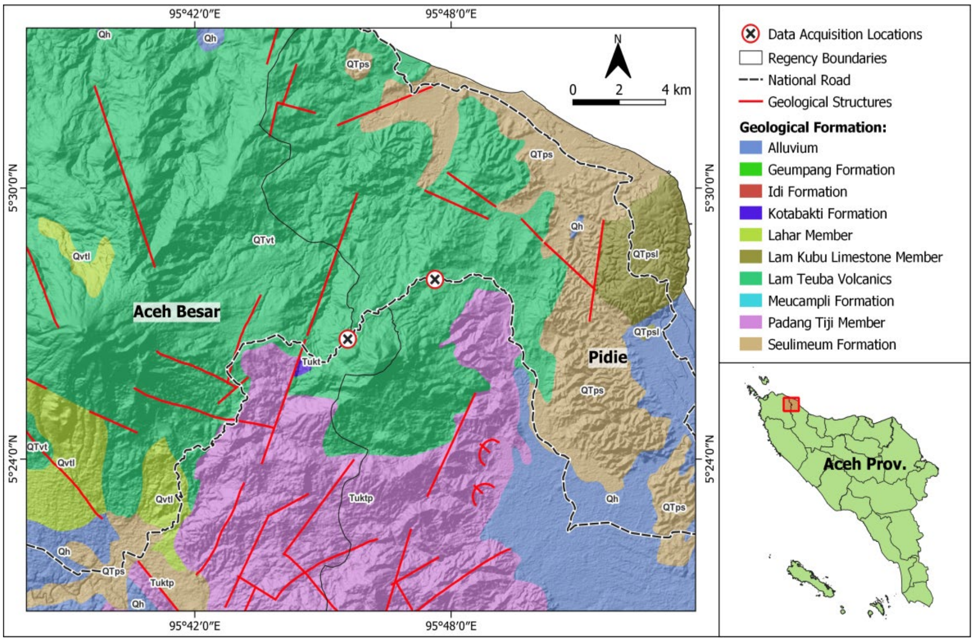

Fig. 1 Geological map of the study area

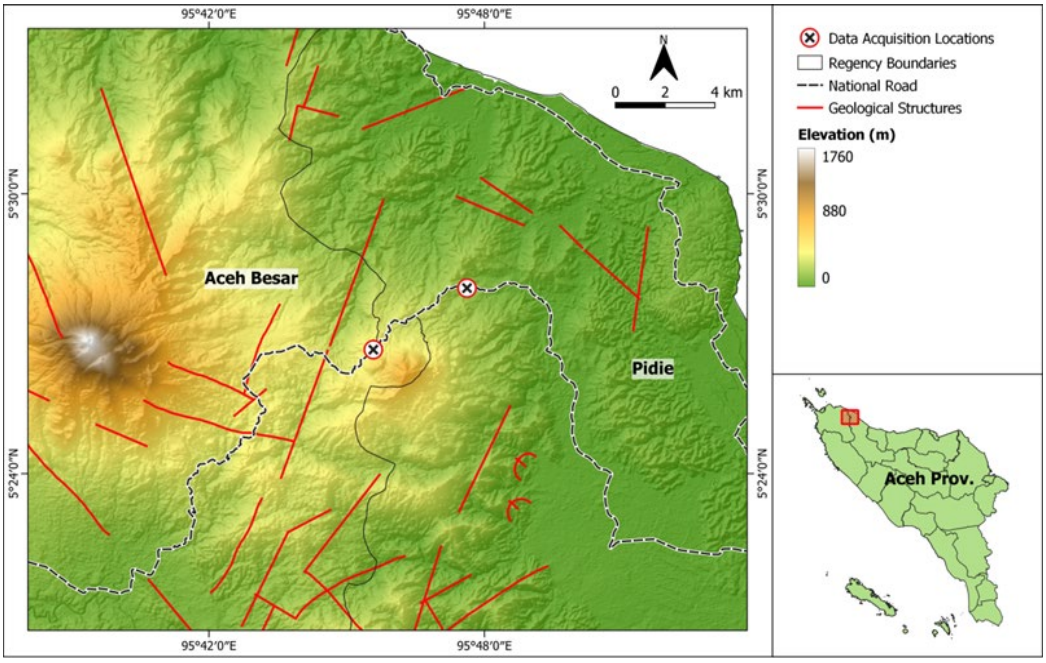

Fig. 2 Digital Elevation Model and Elevation of study area

pumice breccia, agglomerate, and pyroclastic deposits [32]. Near-surface layers consist of unconsolidated Holocene mudflow deposits and loose sediments, indicating ongoing volcanic and fluvial processes.

Topographic conditions derived from the Digital Elevation Model (DEM) (Fig. 2) indicate elevations ranging from 100 to 500 m, with steep slopes and confined valleys that are highly susceptible to landslides [33]. The study site is located approximately 7 km from the active Seulimum segment of the Sumatra Fault, emphasizing the strong tectonic control on slope instability.

3.2 Seismic Methods

Seismic methods are applied to investigate subsurface structures based on wave propagation in elastic media. Seismic velocities are influenced by physical properties such as density, porosity, and lithology [12]. In this study, seismic refraction and MASW were used as active seismic methods with artificial energy sources [20].

3.3 Data Acquisition

Data acquisition was conducted along the Seulawah road using a PASI 16S-24P seismograph. Two survey lines were arranged perpendicular to the slope and spaced 46 m apart, with approximately 5 km between locations. Each line consisted of 24 geophones with 2 m spacing. A 12 Hz geophone was used for seismic refraction, while a 4 Hz geophone was used for MASW. Seismic energy was generated using a 12 lb hammer.

For seismic refraction, shot points were positioned along the line and at offset distances. For MASW, shot points included 12 inline and 2 offset positions to enhance shear-wave detection. Data acquisition geometry and workflow are illustrated in Fig. 3 (seismic refraction) and Fig. 4 (MASW).

3.4 Data Processing and Modelling

Seismic refraction data processing involved first-arrival picking and inversion using SeisImager and PlotRefa software to generate 2D P-wave velocity (Vp) models (Fig. 3). MASW processing included dispersion analysis and inversion to obtain shear-wave velocity (Vs) profiles [34]. Dispersion curves were derived using phase-shift and Fourier Transform methods, relating Rayleigh wave velocity to frequency [21]. The inversion process produced 1D Vs profiles through iterative model fitting [35] as illustrated in Fig. 4.

3.5 Geotechnical Parameter Estimation

Geotechnical and engineering parameters were calculated from Vp and Vs values obtained from seismic refraction and MASW. Elastic parameters,

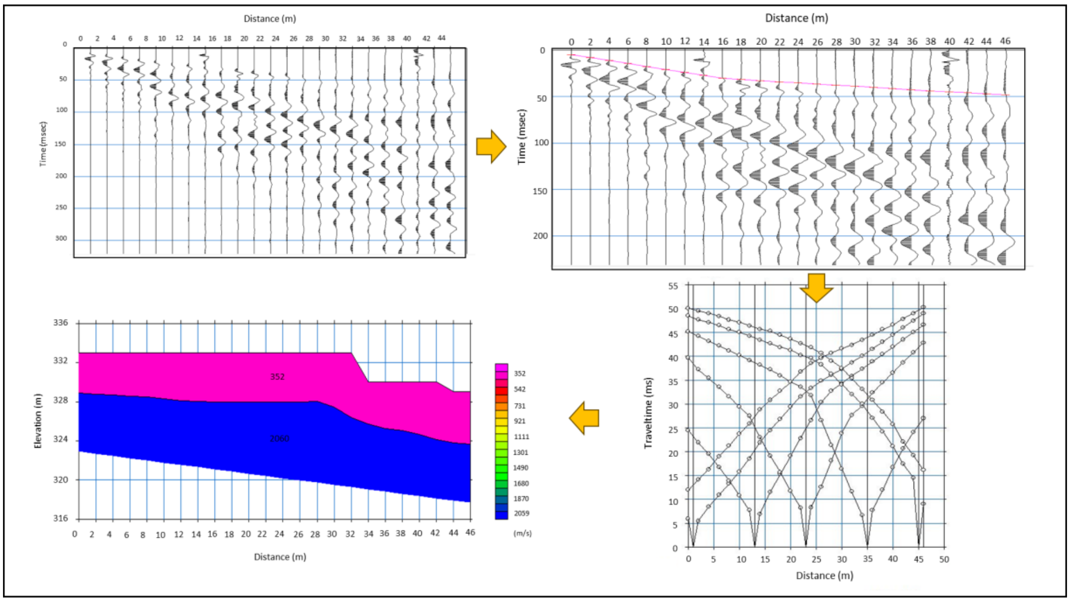

Fig. 3 Processing Steps of seismic refraction method

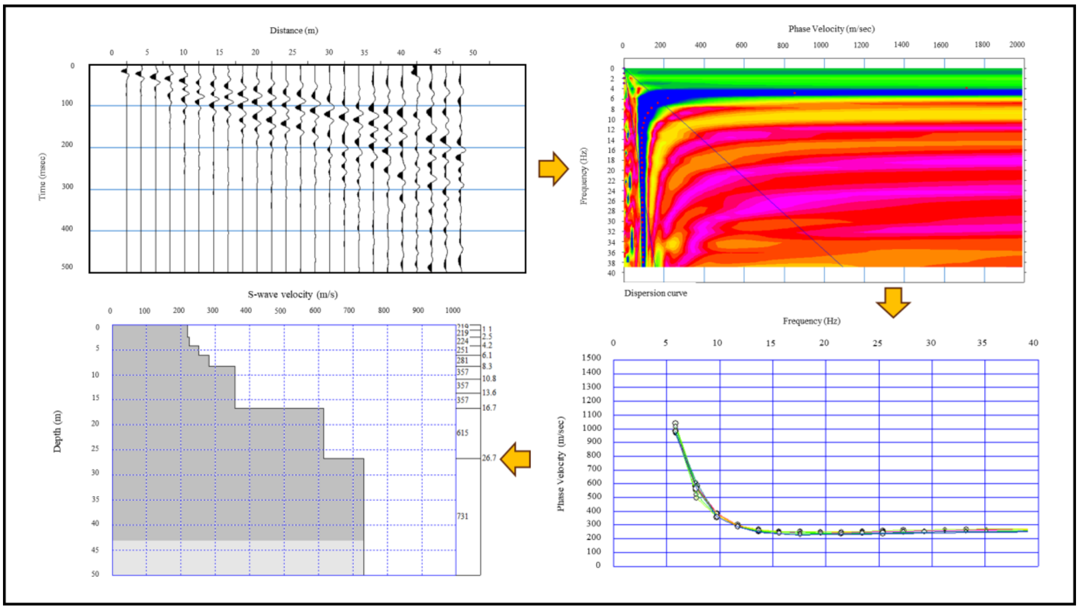

Fig. 4 Processing steps of MASW method

including Young's modulus, bulk modulus, shear modulus, and Poisson's ratio, were derived using established equations [26, 27]. Additional parameters such as stress ratio, density, and ultimate bearing capacity were also estimated [7, 11, 24]. These parameters were used to evaluate subsurface material properties and landslide susceptibility.

4. RESULT AND DISCUSSION

Field observations (Fig. 5) reveal active landslide features, including road subsidence, at both steep-slope sites. Consistent with the DEM (Fig. 2), the geomorphological setting and weak near-surface materials indicate high landslide susceptibility.

4.1 Seismic Refraction and MASW Results

The seismic refraction results at Location 1 (Fig. 6) and Location 2 (Fig. 7) show Vp values ranging from 295 to 2298 m/s, with a penetration depth of approximately 17 m. The Vp models consistently identify three subsurface layers. The upper layer (Vp: 295–1000 m/s) is interpreted as unconsolidated topsoil and sandy gravel. The second layer (Vp > 1000 m/s) corresponds to compact volcanic tuff and breccia, while deeper zones indicate more lithified materials. The Vp contour patterns in Fig. 6 and Fig. 7 follow slope geometry, suggesting structural control by topography.

MASW results at Location 1 (Fig. 6) and Location 2 (Fig. 7) provide Vs profiles with penetration depths up to ~30 m. Based on SNI 1726:2019 classification [36], two main layers are identified. The upper layer (Vs < 350 m/s) represents medium soil, interpreted as loose to moderately compacted materials. The lower layer (Vs: 350–750 m/s) corresponds to dense soil or stiff volcanic deposits. These results, as shown in Fig. 6 and Fig. 7, indicate improved stiffness and reduced settlement potential with depth.

Fig. 5 Landslide condition of study area

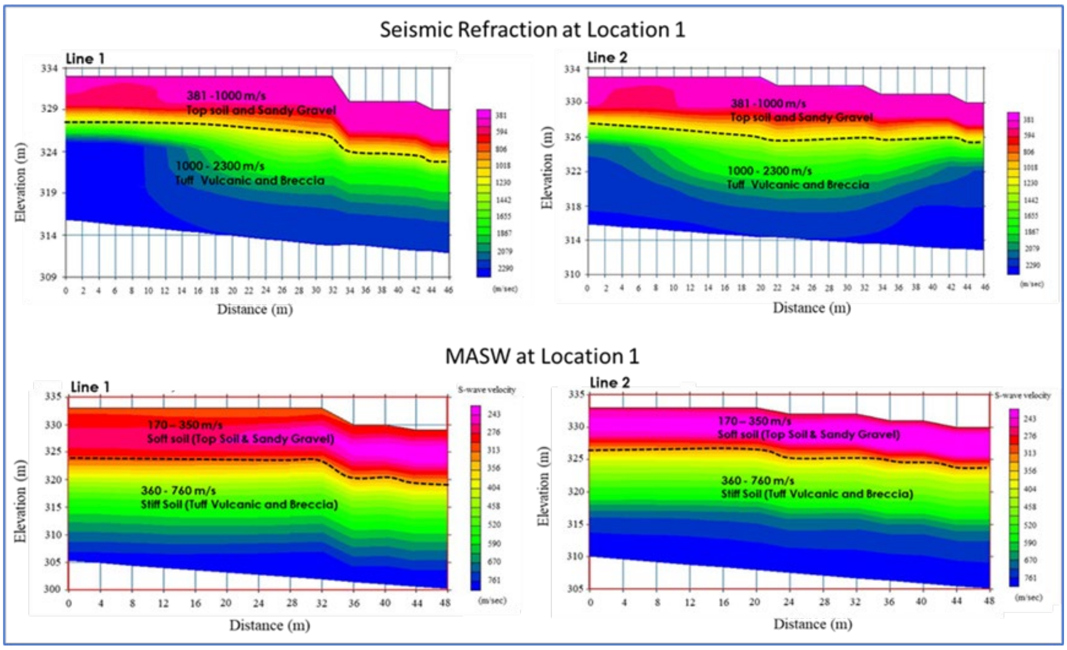

Fig. 6 Result of MASW dan Refraction method at location 1

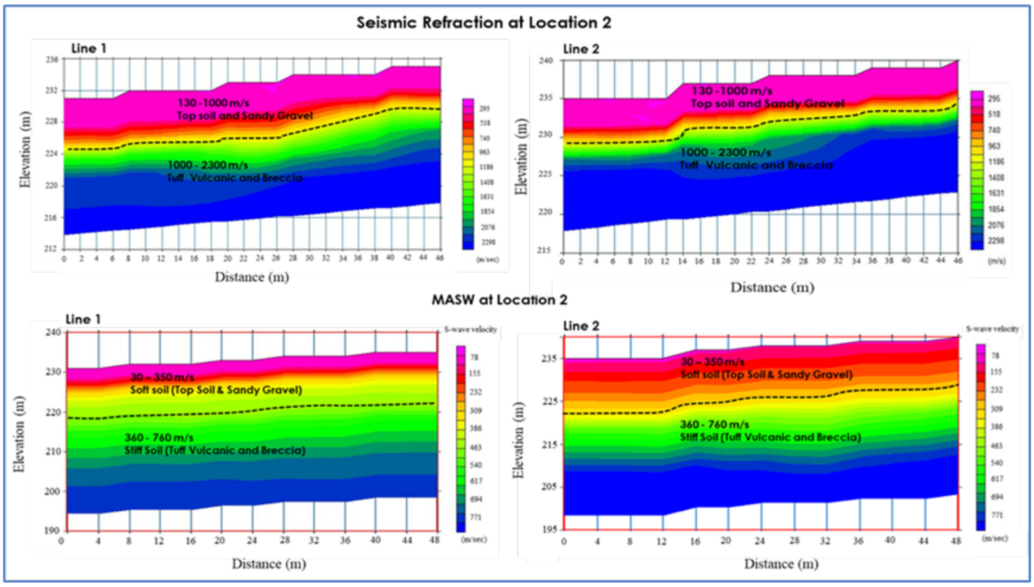

Fig. 7 Result of MASW dan Refraction method at location 2

4.2 Geotechnical Parameter Analysis

The calculated geotechnical parameters at Location 1 (Table 1) and Location 2 (Table 2) indicate a consistent increase in material strength with depth. The shallow layer is characterized by low density (1.73–1.86 g/cm³), low Young's modulus (6.1×10^4–2.7×10^5 Pa), and low bearing capacity (1.94–4.87), indicating weak, unconsolidated materials susceptible to deformation and landslides. In contrast, the deeper layer exhibits higher Vp (up to 2411 m/s), Vs (up to 897 m/s), density (up to 2.92 g/cm³), elastic modulus (up to 6.68×10^6 Pa), and bearing capacity (up to 26.23), indicating dense volcanic rocks with greater stiffness and load-bearing capacity. As shown in Fig. 6 and Fig. 7, the marked contrast between these layers controls slope instability.

Layers with Vp <1000 m/s, Vs <350 m/s, density <1.9 g/cm³, and bearing capacity <5 are interpreted as mechanically weak zones with high landslide susceptibility, whereas higher seismic velocities and engineering parameters indicate competent materials with lower failure potential. Although these parameters were derived from established empirical relationships, the interpreted subsurface models agree with regional geology and field observations, supporting their reliability for first-order geotechnical characterization. Overall, the integrated seismic refraction–MASW approach effectively identifies weak zones and provides a reliable basis for slope stability evaluation and landslide hazard assessment.

Table 1. Results calculation of Geotechnics parameters at Location 1

X	Depth (m)	Vp (m/s)	Vs (m/s)	Density (g/cm³)	Modulus Young (Pa)	Bulk	Shear	Poisson Ration (v)	Strees Ratio	Bearing Capacity
22	333	389	234	1.85	247128	205015	101487	0.22	0.28	4.34
22	332	401	240	1.87	263537	219754	108061	0.22	0.28	4.48
22	331	392	241	1.86	250501	202331	109663	0.17	0.23	4.48
22	330	397	262	1.86	279128	197322	127663	0.10	0.12	4.87
22	329	693	307	2.14	559763	873679	206575	0.37	0.60	6.58
22	327	1452	304	2.58	701296	5249658	237384	0.48	0.91	7.82
22	326	1486	456	2.59	1556660	5316975	537466	0.45	0.81	11.80
22	324	1603	441	2.64	1513550	6398375	519738	0.46	0.85	11.64
22	321	1944	539	2.77	2377057	9852660	816860	0.46	0.84	14.93
22	319	2150	659	2.84	3664344	12182012	1272764	0.45	0.81	18.72
22	316	2167	993	2.85	7668605	11260224	2804492	0.37	0.58	28.25
22	317	2292	881	2.89	6332662	13483999	2240340	0.41	0.70	25.43

Table 2. Results calculation of Geotechnics parameters at Location 2

X	Depth (m)	Vp (m/s)	Vs (m/s)	Density (g/cm³)	Modulus Young (Pa)	Bulk	Shear	Poisson Ration (v)	Strees Ratio	Bearing Capacity
22	237	295	112	1.73	61620	134156	21767	0.42	0.71	1.94
22	237	295	132	1.73	83140	128333	30237	0.37	0.60	2.29
22	236	320	162	1.76	122450	146301	46065	0.33	0.49	2.85
22	235	368	188	1.83	171315	199679	64712	0.32	0.48	3.44
22	234	369	229	1.83	227526	177228	95801	0.19	0.23	4.19
22	233	325	111	1.77	62429	170951	21764	0.43	0.77	1.96
22	232	327	114	1.77	65757	172006	22978	0.43	0.76	2.02
22	231	1880	238	2.75	464190	9591968	155575	0.49	0.97	6.54
22	229	2029	330	2.80	906797	11305247	305028	0.49	0.95	9.24
22	227	2227	378	2.87	1213648	13909872	408579	0.49	0.94	10.82
22	225	2410	585	2.92	2939119	16229095	1000592	0.47	0.88	17.10
22	223	2411	897	2.92	6683568	15225983	2354052	0.42	0.72	26.23

5. CONCLUSION

This study demonstrates that the integration of seismic refraction and MASW effectively characterizes subsurface conditions in landslide-prone areas. Two distinct subsurface layers were identified at both locations. The upper layer (8–11 m depth) exhibits low Vp (295–1000 m/s), Vs (112–350 m/s), density (1.73–1.86 g/cm³), and bearing capacity (1.94–4.87), indicating weak, unconsolidated materials susceptible to slope failure. In contrast, the deeper layer is characterized by higher Vp (up to 2411 m/s), Vs (up to 897 m/s), density (up to 2.92 g/cm³), and bearing capacity (up to 26.23), representing competent volcanic tuff and breccia. The integrated Vp–Vs interpretation and derived engineering parameters effectively distinguish weak and competent subsurface layers, enabling reliable identification of potential slip zones. These findings demonstrate that the combined seismic refraction–MASW approach provides an effective framework for geotechnical characterization and landslide hazard assessment in volcanic terrains.

6. ACKNOWLEDGMENTS

The authors acknowledge the ministry of research, technology, and higher education, indonesia, for financial support provided through the PFR (Penelitian Fundamental Reguler) - 2025 grant scheme (contract number 116/UN11.L1/PG.01.03/DPPM/2025). Special appreciation is also extended to the technical staff, members of the near surface geophysics laboratory, and geophysics students at Universitas Syiah Kuala.

7. REFERENCES

1. Fadhli Z., Wirsya E., Marvita Y., Miska L., Syukri M., and AlFaiz K., Characteristic of Landslide in Seulawah Road KM 80-81 Based on Geophysical Data and Geotechnical Parameters, Jurnal Geosaintek, Vol.11, No.2, 2025, pp.225-238. https://doi.org/10.12962/j25023659.v11i2.5122
2. Bello A., Muztaza N.M., Abir I.A., Zakaria M.T., and Bello J., Geophysical Performance of Subsurface Characterization for Site Suitability in Construction Purpose, Physics and Chemistry of the Earth, Vol.128, 2022, pp.1-20. https://doi.org/10.1016/j.pce.2022.103296
3. Indrawan I.G.B., Tamado D., Abrar M., and Warmada I.W., Mineralogical and Engineering Properties of Soils Derived from In Situ Weathering of Tuff in Central Java, Indonesia, Geosciences, Vol.14, No.8, 2024, pp.1-17. https://doi.org/10.3390/geosciences14080213
4. Adeleke B., Kinuthia J., and Oti J., Strength and Swell Performance of High-Sulphate Kaolinite Clay Soil, Sustainability, Vol.12, No.23, 2020, pp.1-14. https://doi.org/10.3390/su122310164
5. Sieh K. and Natawidjaja D., Neotectonics of the Sumatran Fault, Indonesia, Science, Vol.289, No.5482, 2000, pp.503-507. https://doi.org/10.1126/science.289.5482.503
6. Muksin U., Arifullah A., Simanjuntak A.V.H., Asra N., Muzli M., Wei S., Gunawan E., and Okubo M., Secondary Fault System in Northern Sumatra Evidenced by Recent Seismicity and Geomorphic Structure, Journal of Asian Earth Sciences, Vol.245, 2023, pp.1-20. https://doi.org/10.1016/j.jseaes.2023.105557

7. Muksin U., Irwandi, Rusydy I., Muzli, Erbas K., Marwan and Ismail N., Investigation of Aceh Segment and Seulimeum Fault by Using Seismological Data: A Preliminary Result, Journal of Physics: Conference Series, Vol. 1011, 2018., pp. 1-6. https://doi.org/10.1088/1742-6596/1011/1/012031
8. Gauriau J. and Dolan J., Comparison of Geodetic Slip-Deficit and Geologic Fault Slip Rates Reveals that Variability of Elastic Strain Accumulation and Release Rates on Strike-Slip Faults is Controlled by the Relative Structural Complexity of Plate-Boundary Fault Systems, Seismica, Vol. 3, No. 1, 2024.pp.1-20. https://doi.org/10.26443/seismica.v3i1.1119
9. Syukri M., Anda S.T., Muksin U., Meilianda E., Saad R., Fadhli Z. and Safitri R., Identification of Tsunami Deposit at Meulaboh, Aceh (Indonesia) Using Ground Penetrating Radar (GPR), GEOMATE Journal, Vol. 23, No. 96, 2022, pp.171-178. https://doi.org/10.21660/2022.96.j226
10. Hardiyatmo H.C., Srijono and Karnawati D., Mineralogical and Geochemical Control of Altered Andesitic Tuff upon Debris Slide Occurrences at Pelangan Area, Southern Mountain of Lombok Island, Indonesia, Journal of Applied Geology, Vol. 6, No. 1, 2021, pp.35–47. https://doi.org/10.22146/jag.26953
11. Saad R., Samuel Y.M., Nordiana M.M., Ismail N.A. and Saisin M.M., Magnetics, 2-D Resistivity and Geotechnical Studies for Shallow Subsurface Soil Characterization in Lembah Bujang, Kedah, Jurnal Teknologi (Sciences & Engineering), Vol. 78, No. 7-3, 2016, pp. 123–127. https://doi.org/10.11113/jt.v78.9504
12. Syukri M., Muztaza N.M., Ismail N.A., Fadhli Z. and Saad R., Identifying Shallow Subsurface Characteristics via Compressional to Shear Waves Velocity Ratio (Vp/Vs) from Seismic Refraction Tomography, Jurnal Teknologi (Sciences & Engineering), Vol. 83, No. 1, 2020, pp.67–73. https://doi.org/10.11113/jurnalteknologi.v83.14990
13. Hasanah M., Syamsuddin F., Safitri R., Fadhli Z., Karmel M.E.R. and Syukri M., Analysis of Gravity Anomaly Data for Identification of Mineral Distribution Prospects in the Kuta Cot Glie Area, Aceh Besar, IOP Conference Series: Earth and Environmental Science, Vol. 1356, 2024, pp.1-9. https://doi.org/10.1088/1755-1315/1356/1/012118
14. Santosa I., Sulaksana N., Yuningsih E.T. and Zakaria Z., The Sliding Surface Determination of a Deep-Seated Landslide on Cisumdawu Highway, West Java, Based on the Electrical Resistivity Tomography, Indonesian Journal on Geoscience, Vol. 11, No. 2, 2024, pp.189–199. https://doi.org/10.17014/ijog.11.2.189-199
15. Syukri M., Fadhli Z., Hasibuan P., Saputra H. and Safitri R., Recent Developments in the Use of Geoelectric Surveys for Investigating Causes of Road Pavement Failure: A Case Study along Darussalam Road, Aceh, Indonesia, Ecological Engineering & Environmental Technology (EEET), Vol. 26, No. 10, 2025, pp.128–139. https://doi.org/10.12912/27197050/210524
16. Syukri M., Fadhli Z., Hasibuan P., Saputra H. and Safitri R., Geophysical and Geotechnical Study for Assessing the Potential of Landslide Disasters: A Case Study in Krueng Sabet, Aceh Jaya, Indonesia, GEOMATE Journal, Vol. 29, No. 135, 2025, pp.190–198. https://doi.org/10.21660/2025.135.5199
17. Rusydy I., Al-Huda N., Fahmi M. and Effendi N., Kinematic Analysis and Rock Mass Classifications for Rock Slope Failure at USAID Highways, Structural Durability & Health Monitoring, Vol. 13, No. 4, 2019, pp.379–398. https://doi.org/10.32604/sdhm.2019.08192
18. Saputra H., Fadhli Z., Safitri R. and Syukri M., Integrated Geophysical Analysis for Landslide Risk Mitigation: A Case Study on the Weak Zone Area of Jantho-Lamno Route, Aceh, Indonesia, GEOMATE Journal, Vol. 26, No. 113, 2024, pp.41–49. https://doi.org/10.21660/2024.113.4184
19. Mi B., Xia J., Bradford J.H. et al., Estimating Near-Surface Shear-Wave-Velocity Structures via Multichannel Analysis of Rayleigh and Love Waves: An Experiment at the Boise Hydrogeophysical Research Site, Surveys in Geophysics, Vol. 41, 2020, pp.323–341. https://doi.org/10.1007/s10712-019-09582-4
20. Ning L., Dai T., Liu Y., Xi C., Zhang H. and Zhou C., Application of Multichannel Analysis of Passive Surface Waves Method for Fault Investigation, Journal of Applied Geophysics, Vol. 192, 2021, pp.1-19. https://doi.org/10.1016/j.jappgeo.2021.104382
21. Rahimi S., Wood C.M. and Teague D.P., Performance of Different Transformation

Techniques for MASW Data Processing Considering Various Site Conditions, Near-Field Effects, and Modal Separation, Surveys in Geophysics, Vol. 42, No. 5, 2021, pp.1197–1225. https://doi.org/10.1007/s10712-021-09657-1
22. Fadhli Z., Miska L., Marvita Y., Ismail N.A., Elhidayah Ismail N. and Wirsya E., Integration of S-Wave Value, N-SPT and Soil Bearing Capacity for Landslide Analysis, The Iraqi Geological Journal, Vol. 58, No. 2B, 2025, pp.36–50. https://doi.org/10.46717/igj.2025.58.2B.3
23. Olutoki J.O., Zhao J., Siddiqui N.A., Elsaadany M., Haque A.E., Akinyemi O.D., Said A. and Zhao Z., Shear Wave Velocity Prediction: A Review of Recent Progress and Future Opportunities, Energy Geoscience, Vol. 5, No. 4, 2024, pp.1–19. https://doi.org/10.1016/j.engeos.2024.100338
24. Gardner G.F., Gardner L.W. and Gregory A.R., Formation Velocity and Density: The Diagnostic Basics for Stratigraphic Traps, Geophysics, Vol. 39, No. 6, 1974, pp.770–780. https://doi.org/10.1190/1.1440465
25. Shi F., Wang Y. and Liu X., Study on Calculation Method of Compressional Velocities Based on Field Well Logs, International Journal of Geosciences, Vol. 7, 2016, pp.928–937. https://doi.org/10.4236/ijg.2016.77069
26. Fat-Helbary R.E.S., El-Faragawy K.O. and Hamed A., Soil Geotechnical Characteristics for Seismic Risk Mitigation at the Southern Extension of Marsa Alam City, Egypt, NRIAG Journal of Astronomy and Geophysics, Vol. 8, No. 1, 2019, pp.1–14. https://doi.org/10.1080/20909977.2019.1588676
27. Lowrie W. and Fichtner A., Fundamentals of Geophysics, 3rd ed., Cambridge University Press, 2020, pp.1–411
28. Keaton J.R., Bulk Modulus, in Bobrowsky P. and Marker B. (Eds.), Encyclopedia of Engineering Geology, Encyclopedia of Earth Sciences Series, Springer, Cham, 2017, pp.1–2. https://doi.org/10.1007/978-3-319-12127-7_38-1
29. Abudeif A.M., Raef A.E., Moneim A.A., Mohammed M.A. and Farrag A.F., Dynamic Geotechnical Properties Evaluation of a Candidate Nuclear Power Plant Site (NPP): P- and S-Waves Seismic Refraction Technique, North Western Coast, Egypt, Soil Dynamics and Earthquake Engineering, Vol. 99, 2017, pp.124–136. https://doi.org/10.1016/j.soildyn.2017.05.006
30. Mohammed M.A., Abudeif A.M. and Abd El-Aal A.K., Engineering Geotechnical Evaluation of Soil for Foundation Purposes Using Shallow Seismic Refraction and MASW, Journal of African Earth Sciences, Vol. 162, 2020, pp.1-20. https://doi.org/10.1016/j.jafrearsci.2019.103721
31. Zhong J., Hou C. and Yang X., Bearing Capacity of Foundations Resting on Rock Masses Subjected to Rayleigh Waves, Soil Dynamics and Earthquake Engineering, Vol. 167, 2023, pp.1-20. https://doi.org/10.1016/j.soildyn.2023.107791
32. Zaini N., Yanis M., Marwan, Isa M. and Meer F.V.D., Assessing of Land Surface Temperature at the Seulawah Agam Volcano Area Using the Landsat Series Imagery, Journal of Physics: Conference Series, Vol. 1825, No. 1, 2021, pp1-8. https://doi.org/10.1088/1742-6596/1825/1/012021
33. Susetyo D.B., Vertical Accuracy Assessment of Various Open-Source DEM Data: DEMNAS, SRTM-1, and ASTER GDEM, Geodesy and Cartography, Vol. 49, No. 4, 2023, pp.209–215. https://doi.org/10.3846/gac.2023.18168
34. Hamed A., Fat-Helbary R.E. and Gowad A.M.A., Active and Passive Seismic Data Integration for Delineating the Near-Surface Velocity Models at Ras Samadai Area, Red Sea-Egypt, Modeling Earth Systems and Environment, Vol. 10, No. 4, 2024, pp.5309–5327. https://doi.org/10.1007/s40808-024-02065-5
35. James N., Sitharam T.G., Padmanabhan G. and Pillai C.S., Seismic Microzonation of a Nuclear Power Plant Site with Detailed Geotechnical, Geophysical and Site Effect Studies, Natural Hazards, Vol. 71, No. 1, 2014, pp.419–462. https://doi.org/10.1007/s11069-013-0919-0
36. Badan Standardisasi Nasional, SNI 1726:2019: Tata Cara Perencanaan Ketahanan Gempa untuk Struktur Bangunan Gedung dan Nongedung, 2019, pp.1–254. https://sitaba.pu.go.id/publikasi/6977fb4f-d02f-4fd0-a857-65219c38f24e